Feasibility Study of a Radical Vane-Integrated Heat Exchanger for Turbofan Engine Applications

Proceedings of ASME Turbo Expo 2020
Turbomachinery Technical Conference and Exposition
GT2020
June 22-26, 2020, London, England

GT2020-15243

FEASIBILITY STUDY OF A RADICAL VANE-INTEGRATED HEAT EXCHANGER FOR TURBOFAN ENGINE APPLICATIONS

Isak Jonsson, Carlos Xisto, Hamidreza Abedi, Tomas Grönstedt

Department of Mechanics and Maritime Sciences,
Chalmers University of Technology
Gothenburg SE-41296, Sweden

Marcus Lejon

GKN Aerospace
Trollhättan SE- 461 38, Sweden

ABSTRACT

In the present study, a compact heat exchanger for cryogenically fueled gas turbine engine applications is introduced. The proposed concept can be integrated into one or various vanes that comprise the compression system and uses the existing vane surface to reject core heat to the cryogenic fuel. The requirements for the heat exchanger are defined for a large geared-turbofan engine operating on liquid hydrogen. The resulting preliminary conceptual design is integrated into a modified interconnecting duct and connected to the last stage of a publicly available low-pressure compressor geometry. The feasibility of different designs is investigated numerically, providing a first insight on the parameters that govern the design of such a component.

Keywords: Hydrogen; Heat Management; Compressor; Interconnecting duct; CFD

NOMENCLATURE

λ	Pressure loss coefficient
L	S-Duct length (m)
r	Mean radius (m)
LH2	Liquid hydrogen
LPC	Low-pressure compressor
ICD	Interconnecting compressor duct
IGV	Inlet guide vane
HEX	Heat exchanger
HPC	High-pressure compressor
OGV	Outlet guide vane
STRUT	Structure vane

INTRODUCTION

The density of liquid hydrogen (LH2), at the normal boiling point, is two times higher than that of highly compressed gaseous hydrogen. This makes LH2 the prime candidate for hydrogen storage in aviation. However, LH2 is stored at cryogenic temperatures and therefore requires adequate insulation, as well as the integration of heat exchangers (HEX) along the fuel line to warm up the hydrogen on its way to the combustion chamber.

Preheating the fuel from a cryogenic condition of around 25 K possibly all the way up to 800-1000 K requires about up to 14 MJ/kg, *i.e.* about 10% of the standard state combustion value of the fuel. Conversely for the air flowing into the engine, even if a typical fuel air ratio for hydrogen combustion will not be more than 1%, this could potentially amount to around a 140 K change in temperature of the working gas.

Ideally, the required heat exchangers are strategically placed in the engine core to result in optimum heat management, targeting improvements in the engine efficiency and increase of component durability as well as to reduce emissions. Moreover,

the combination of hydrogen's high specific heat with cryogenic temperatures results in a formidable cooling capacity that can be explored by more compact HEX solutions.

The present work numerically investigates a novel concept of a compact compressor vane-integrated heat exchanger, for application in cryogenically fueled gas turbine engines. The main goal of the paper is to provide a first insight on the design challenges and potential benefits. The baseline engine used for establishing the HEX requirements is a large geared turbofan, operating on liquid hydrogen. The HEX aero-thermal performance is first estimated using zero-dimensional models and Chalmers in-house gas turbine performance tool GESTPAN. After, the conceptual design of a vane-integrated HEX is developed and integrated into the interconnecting duct located after a three-stage low-pressure compressor. The multi-stage compressor with the integrated HEX is evaluated using steady-state computational fluid dynamics. The present paper only investigates the feasibility of the proposed concept with respect to its aerodynamic performance. In practice, this means that the computations will only be made to estimate the HEX performance in terms of total pressure loss and the potential enhanced radial flow turning capability.

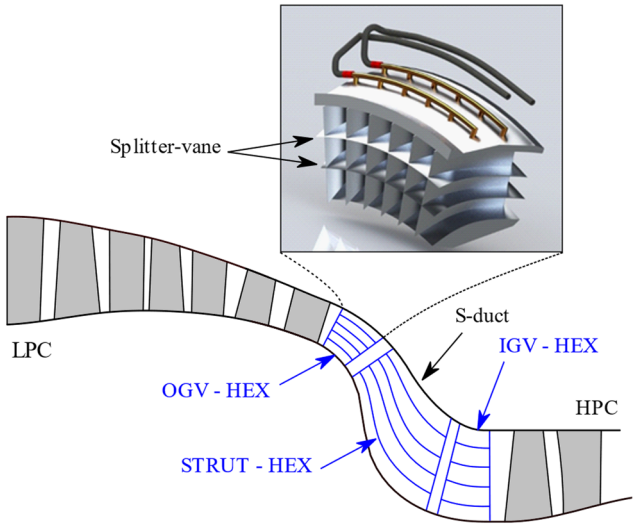

FIGURE 1: ILLUSTRATION OF A POSSIBLE COMPOUND HEX ARRANGEMENT.

Outlet Guide Vane Heat Exchanger

The main task of the fuel supply system is to feed the right amount of fuel, with appropriate pressure, to the combustion chamber. This requires a set of fuel pumps (boost pumps at each tank and high-pressure pump at the engine), valves, and a fuel control system to adjust the fuel flow for a given engine rating. For the case of cryogenic fuels, particularly liquid hydrogen stored at 20K, the inclusion of heat exchangers along the fuel line is also a requirement to deliver the fuel to the combustor chamber at adequate temperature.

In the present section a compact vane integrated heat exchanger is introduced. The heat exchanger can be integrated into one or various vanes that comprise the compression system and uses the existing vane surface to reject core heat to the hydrogen fuel. Additional profiled plates can be added spanwise to increase the available surface area, see Figure 1. The additional spanwise distributed plates (splitter-vanes) will lead to additional pressure losses in the engine core but can also be designed to enhance the radial turning capability of the vane. The radial turning capability can allow for a reduction of engine length and weight by reducing the axial length of the transition S-duct between the low- and high-pressure compressors.

The concept illustrated in Figure 1 shows a possible arrangement of a compound heat exchanger, where the first HEX is placed at the low-pressure compressor outlet guide vane (OGV), a second HEX is integrated into the STRUT, and a third HEX is included in the high-pressure compressor inlet guide vane (IGV). Such an arrangement allows for the OGV-HEX to turn the flow radially downwards into the aggressive S-duct, and for the STRUT- and IGV-HEX to straighten the flow towards the high-pressure compressor first stage.

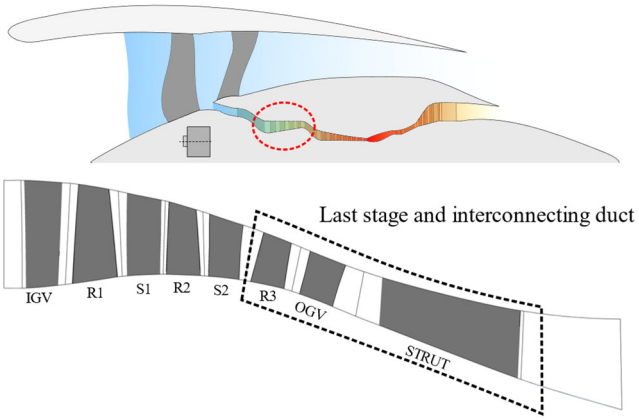

FIGURE 2: 3-STAGE VINK LOW-PRESSURE COMPRESSOR

BASELINE HIGH SPEED VINK LPC

The baseline compressor geometry is a lightly loaded high-speed low-pressure compressor (LPC) with a design pressure ratio of 2.8 [1]. The LPC is part of a year 2035 representative large geared turbofan engine, providing a thrust of 70,000 lbf at sea level static conditions. The engine performance are in line with project ENABLEH2 long-range application and therefore the operating conditions of the high-speed LPC are considered adequate for the problem in hand.

The multidisciplinary design of the compressor was performed by a consortium of Swedish universities in order to demonstrate that within Sweden the joint capability of achieving

an aeromechanical design of a modern compressor from a clean slate exists. The CAD geometry for the compressor is publicly available for download[1]. Only the last stage of the compressor, comprising the rotor number three (R3), the outlet-guide-vane (OGV) and the interconnecting S-duct including the STRUT, are modelled in the present work. However, the inlet boundary conditions at the R3 inlet were obtained from a full simulation of the entire three-stage compressor. Moreover, in order to analyze the aerodynamic benefits of the proposed vane-HEX, the duct in the VINK compressor geometry is replaced by a more aggressive S-duct.

Interconnecting compressor duct

In a multi-spool gas turbine, annular interconnecting ducts (ICD) are used to connect the low/intermediate-pressure compressor to the high-pressure compressor. The duct is commonly referred as S-ducts due to the radial offset required by the different compressor spools. From an aero-perspective the ICD should be designed to transfer the flow radially with minimal losses and to provide a uniform temperature and pressure distribution at the HPC inlet. The designer will also aim for a shorter duct in axial length to reduce the engine and nacelle length, therefore reducing weight and drag. In modern gas turbine engines, the progressive increase in overall pressure ratio and bypass-ratio leads to larger radial offset between the different parts of the compression system, which in turn requires more aggressive duct designs.

Configuration 1 S-duct

In the present work, the original duct in the VINK compressor is replaced by a more aggressive design. This duct is depicted in Figure 3 with a green dash-dot line. In the present work, the only requirement for such a duct is that it should be separation and shock free. No attempt was made to optimize the hub and shroud lines or the STRUT and OGV profiles.

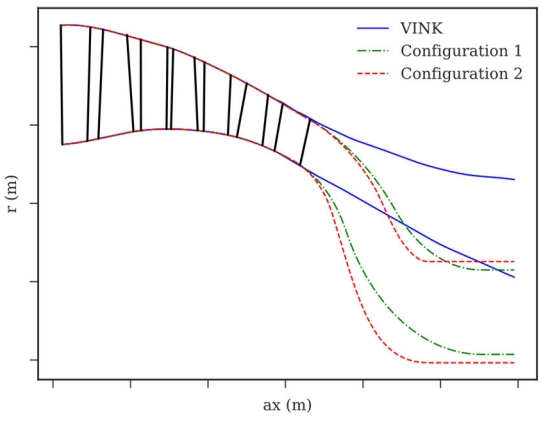

FIGURE 3: HUB AND SHROUD PROFILES OF THE INVESTIGATED DUCT DESIGNS TOGETHER WITH THE ORIGINAL VINK DUCT.

[1] https://github.com/nikander/VINK

Configuration 2 S-duct

With the aim to demonstrate the enhanced aerodynamic capability of the proposed HEX-OGV with respect to radial turning, configuration 2 is introduced. Contrary to the previous design, the configuration 2 S-duct is expected to lead to flow separation with a conventional OGV and STRUT designs. The duct hub and shroud profiles are again shown in Figure 3 (red dash lines). The design of configuration 2 was mainly achieved by shortening the axial length of the previous configuration 1 duct while keeping the same radial shift. The increase in area ratio is driven by the requirement of having a shock free design.

PRELIMINARY CONCEPTUAL DESIGN

The main purpose of this section is to present the methods and the motivation behind the preliminary design of the proposed heat exchanger concept. It starts by estimating what the heat exchanger requirements are for a given system level performance. After, the rationale leading to the different duct designs is described. The section ends with a description of the numerical setup and assumptions employed to analyze the different designs.

Design requirements

The requirements for the proposed vane-integrated HEX are initially predicted using Chalmers university in-house propulsion simulation tool called GESTPAN (GEneral Stationary and Transient Propulsion ANalsysis) [2]. GESTPAN is a generalized simulation system for the prediction of gas turbine performance in design, off-design and transient conditions. GESTPAN has been extensively used and validated across several gas turbine aero-engine applications [3-7].

At this stage GESTPAN is only used to down-select the most promising concepts of HEX integration within the system and to predict the HEX performance using literature correlations for heat-transfer and pressure losses across different types of heat exchangers.

Preliminary results show that for a large geared turbofan operating with liquid hydrogen, the heat transfer between the core flow and the fuel can be as high as 1MW at take-off conditions if the HEX is placed between the low- and high-pressure compression systems. At hot day take-off conditions, the present LPC delivery temperature can be as high as 450 K, and for an exit Mach number of 0.5 the resulting average heat transfer coefficient for the STRUT-vane, predicted using fully turbulent flat plate correlations, is approximately 600 Wm^2/K. If a wall temperature of about 180 K is assumed, the required area to reject 1MW amounts to approximately 6 m^2. The total area of the 8 STRUT vanes is about 0.37 m^2. Each splitter-vane provides a wetted area of approximately 0.8 m^2, the hub and shroud surface area can also be used to exchange heat, giving another

extra 0.8 m^2. This means that the if the HEX is to be placed only in the STRUT, it will require at least six spanwise distributed splitter vanes. In order to simplify the problem and to better identify the challenges of such design, the STRUT is modified to only include a single splitter-vane, placed at approximately mid-span, see Figure 4.

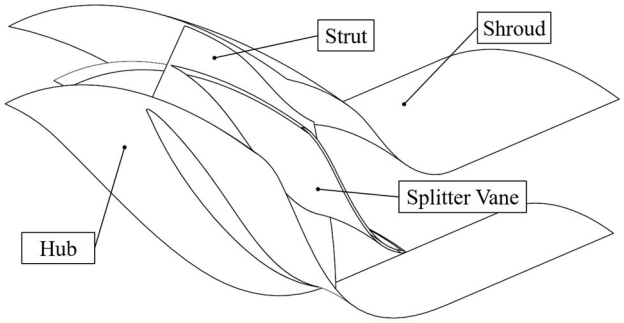

FIGURE 4: ISOMETRIC VIEW OF THE STRUT-HEX CONCEPT INVESTIGATED IN THE PRESENT PAPER.

Blade profiling and duct parameterization

An in-house blade profiling tool is used to generate the vane-HEX profile and to parameterize the interconnecting duct. Two design iterations, including the STRUT-HEX vane, are investigated in the present paper, see Figure 5. The first design, denoted as HEX-1, is based on the configuration 2 duct, with the inclusion of a modified STRUT-HEX concept illustrated in Figure 4. The shroud line is also slightly modified to compensate for the inclusion of the splitter-vane, see the red dot-dash line in Figure 5. Moreover, the splitter-vane leading edge alignment, is based on a stream-line prediction obtained for the configuration 2 duct.

The second design (HEX-2) is a result of a first design iteration after analyzing the results obtained with HEX-1. In HEX-2 the shroud line is further moved radially upwards (dashed blue line in Figure 5) in order to diffuse the flow before and inside the S-duct to simplify the HEX design. Moreover, the HEX-2 splitter vane alignment assumes that the incoming flow is normal to the OGV-duct interface.

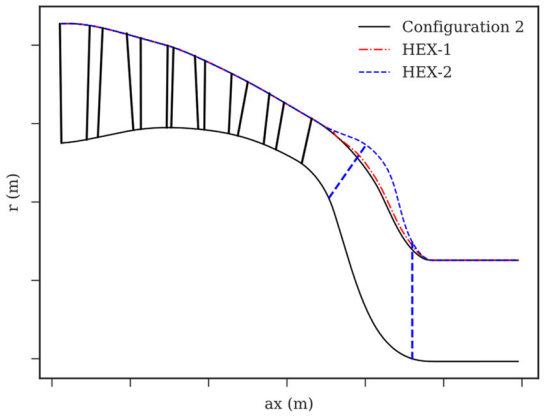

FIGURE 5: HUB AND SHROUD PROFILES OF THE INVESTIGATED HEX DUCT DESIGNS.

Numerical setup

Figure 6 shows the numerical domain used to estimate the aerodynamic performance of the entire system. The simulations are run in ANSYS CFX steady-state solver and mixing-plane interfaces are used to connect the different single-passage domains (R3-OGV-S-duct). Turbulence is predicted using the $k-\omega$ SST model. Near the walls the grid is adequately refined for the usage of wall functions. The grid resolution used in the different domains is also shown in Figure 6. In the duct upstream components, a fixed grid resolution of approximately 230,000 nodes was set for the R3 and 244,000 nodes for the OGV. In the duct domain the resolution was modified for each design ranging from 300,000 nodes (baseline case) to 12 million nodes (Hex-2 case). In the present work the aim is to provide an insight on the feasibility of the concept as well as to investigate what are the parameters governing the design of the vane-integrated HEX. The CFD setup is not suitable to capture heat transfer and the correct location and intensity of separated flows. Still, the usage of wall functions should give an acceptable level of accuracy at this stage in design, with respect to the prediction of secondary flows and overall component losses.

Regarding boundary conditions, at R3 inlet, total pressure and total temperature profiles are imposed, together with flow direction and turbulence intensity. The inlet profiles were obtained from a complete simulation of the entire low-pressure compressor. At the exit of the compressor (S-duct outlet), static pressure is imposed. Since different duct designs are investigated different outlet static pressures are expected to lead to different compressor operating conditions. Therefore, in order to obtain comparable results between the different designs, the static pressure at the outlet is modified until similar operating conditions were obtained at the OGV exit plane. The walls are treated as non-slip and adiabatic, as heat transfer in this context is not within the scope of the present paper.

Convergence was confirmed by inspecting the RMS value of all residuals and by monitoring the variation in corrected mass flow, pressure ratio and efficiency of the compressor.

RESULTS

The aim of the present section is to investigate the feasibility of the proposed designs with respect to S-duct and compressor aerodynamics. The performance of the baseline compressor operating with duct configurations 1 and 2 is first analyzed. After, the two design iterations for the STRUT-HEX vane are

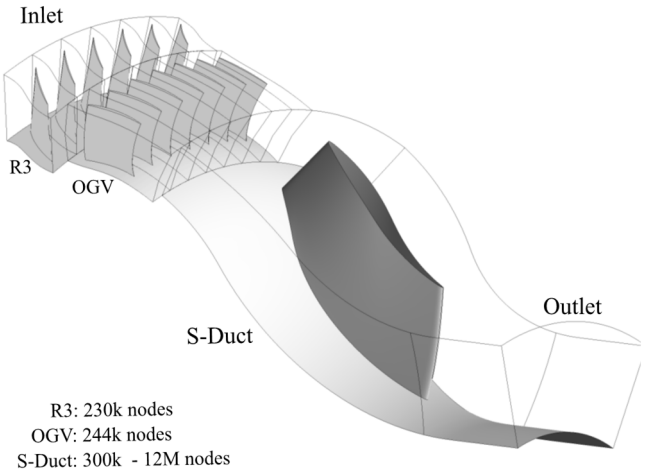

FIGURE 6: ILLUSTRATION OF THE NUMERICAL DOMAIN USED TO ESTIMATE THE AERODYNAMIC PERFOMANCE.

analyzed and compared with respect to duct performance and flow uniformity.

Baseline compressor

The baseline compressor characteristics, obtained with configurations 1 and 2, at nominal rotational speed, are presented in Figure 7. The speed lines show polytropic efficiency and total pressure ratio, calculated between the R3 inlet and OGV outlet, as a function of corrected mass flow. The impact of both ducts on the compressor characteristics is very similar when operating up to a corrected mass flow of 48 kg/s. The difference in choking point is due to the increase in OGV back-pressure for the configuration 2 duct design. Still, the S-duct performance results that are presented throughout the paper are obtained for a compressor pressure-ratio of approximately 1.35 and corrected mass flow of 47.8 kg/s and are therefore assumed to be comparable in terms S-duct inflow conditions.

In Figure 8 the normalized axial velocity contour plots obtained for the baseline compressor operating with duct configurations 1 (a) and 2 (b) are presented. Iso-surfaces representing regions of low axial momentum are also included to identify flow separation. The results in Figure 8-a) show that the configuration 1 is separation free and that the interaction between the STRUT low momentum boundary layer with the radial pressure gradient leads to the occurrence of two counter-rotating corner vortices in the outlet plane. The different intensity of the corner vortices is due to a residual OGV swirl outlet angle.

In Figure 8-b) the results obtained with the configuration 2 duct show flow separation in some portions of the hub and shroud. At the hub, the separation is caused by the adverse pressure gradient in the lower region of the duct. On the other hand, the separation in the shroud corner is caused by the excessive turning. Similar corner vortices of larger intensity are also formed in the configuration 2 duct. Also, in the hub, the interaction between the STRUT corner vortical structures and the

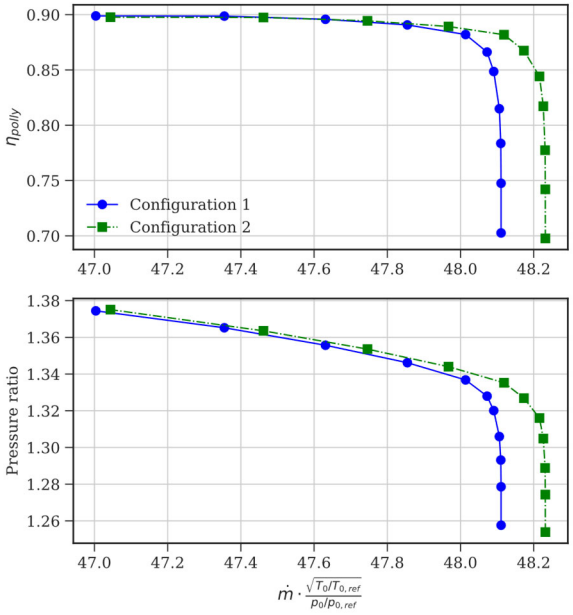

FIGURE 7: COMPRESSOR PERFORMANCE MAP.

primary flow results in an increase of separation flow in the vicinity of the STRUT. It is reminded that in all the test cases, wall functions are applied to model the boundary layer. Hence, results obtained with respect to secondary flows and flow separation should be investigated with care. A more detailed study with fully resolved boundary layer should follow to properly investigate the interaction of different flow mechanism and their impact on the duct performance.

In Table 1 the performance of the two ducts is compared in terms of mass-weighted pressure loss coefficient, λ:

$$\lambda = \frac{p_{0,out} - p_{0,in}}{p_{0,in} - p_{in}} \qquad (1)$$

Where p_0 and p are the mass averaged total and static pressure, respectively, computed at the duct inlet (*in*) and outlet (*out*) planes. The duct performance data is given relative to the reference case (configuration 1). The results show that a 60% increase in pressure loss coefficient is computed when configuration 1 is replaced by the configuration 2 S-duct.

TABLE 1: DUCT LOSSES

	λ/λ_{ref}
Configuration 1	1.0
Configuration 2	1.59
HEX-1	6.31
HEX-2	4.07

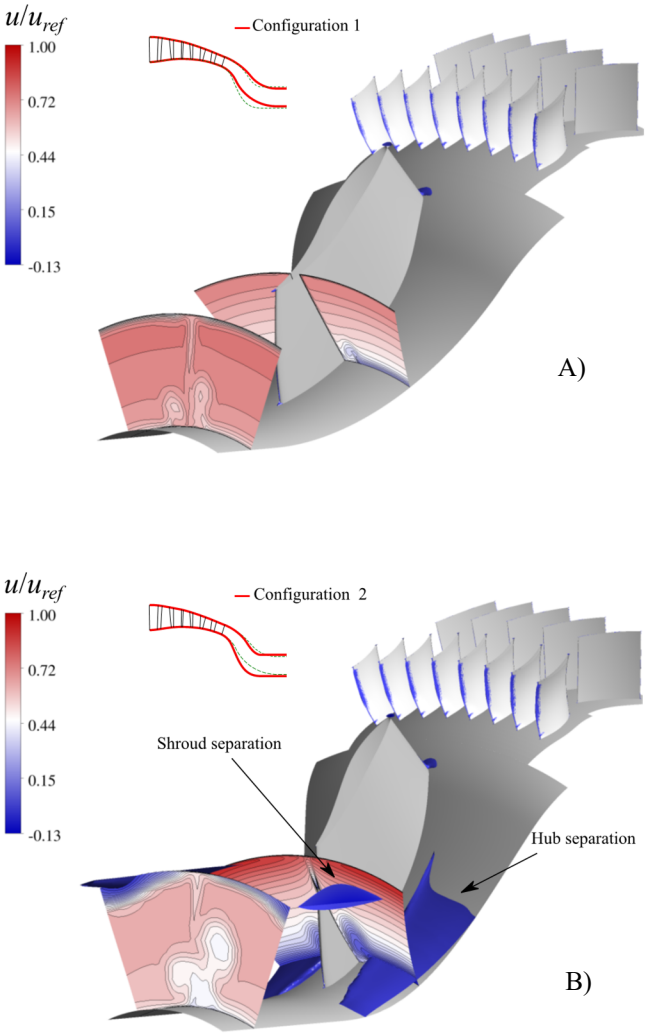

FIGURE 8: NORMALIZED AXIAL VELOCITY COMPUTED FOR CONFIGURATION 1 (A) AND CONFIGURATION 2 (B) DUCT DESIGNS. THE ISO-SURFACE SHOWS REGIONS OF FLOW SEPARATION.

Vane-integrated heat exchanger

Figure 9 shows the normalized axial velocity contour plots obtained for HEX-1 and HEX-2 designs. In the HEX-1 design the duct shroud and hub lines are similar to the configuration 2 duct, with only a minor deviation in the shroud line. The normalized axial velocity results for the HEX-1 design, given in Figure 9-a), show that the inclusion of the splitter-vane suppressed the flow separation in the hub region. However, a much stronger separation is now observed in the splitter-vane suction side. Moreover, the separation also increased in intensity at the shroud. A closer inspection into the Mach number contour plots of Figure 10-a), computed at a given tangential plane, show that the separation in the splitter-vane suction side is caused by excessive incidence as well as the occurrence of a strong shock in the leading edge. The separation in the shroud corner is again due to the excessive turning but it is now amplified by the occurrence of a strong shock.

The HEX-2 design resulted from an attempt to reduce the duct velocities in the upper side of the splitter-vane. The splitter-vane leading edge is also re-aligned assuming that the incoming flow is normal to the OGV-duct interface. The normalized axial velocity contour plots and separation iso-surfaces are shown for HEX-2 in Figure 10-b). When compared to HEX-1 the results now show that the separation in the splitter-vane suction side is significantly reduced. The reduction is related to a better alignment between the leading-edge with the incoming flow as well as a reduction of the leading-edge shock intensity. This behavior is better illustrated in the Mach number contour plots shown in Figure 10-b). It is also visible in both plots that the intensity of the shroud corner separation is also reduced for the HEX-2 design due to a better redistribution of flow in the suction side of the splitter vane and local reduction of corner shock intensity.

Both designs provide a high degree of pressure losses when compared to the reference configuration 1 duct. In Table 1 the pressure loss coefficient increased 6-fold relative to the reference duct design. However, within the second iteration (HEX-2) the pressure loss coefficient was reduced by 36%. This clearly indicates that such a concept is feasible and there is significant margin for improvement.

CONCLUSION

In the present paper the feasibility of a STRUT-vane-integrated heat exchanger was evaluated using numerical tools. The HEX requirements were computed with Chalmers in-house gas turbine performance tool. The predicted required wetted area, for a heat rejection of about 1MW, is approximately 6 m^2. For the present STRUT design the total wetted area of 8 vanes is 16 times lower than the required value. Hence, additional wetted area surface could be added with the aid of spanwise distributed splitter-vanes. For the present study, only one splitter-vane was added at approximately mid-span to simplify the initial design problem. Two design iterations, including the splitter-vane, were introduced and investigated. In the first design (HEX-1) the existing configuration 2 duct was kept. Such design led to a suppression of flow separation in the hub, but also resulted in prohibited amounts of flow separation in the suction side of the splitter-vane and shroud corner. A second iteration (HEX-2) was therefore introduced in order to suppress the aforementioned flow separation regions. The new design led to a decrease in flow separation at the splitter-vane and shroud regions. However, the excessive amount of diffusion employed led to additional separated flow in the hub. Still, the reduction in pressure loss coefficient for only one iteration was about 36% relative to HEX-1, revealing that a feasible design is probably within range.

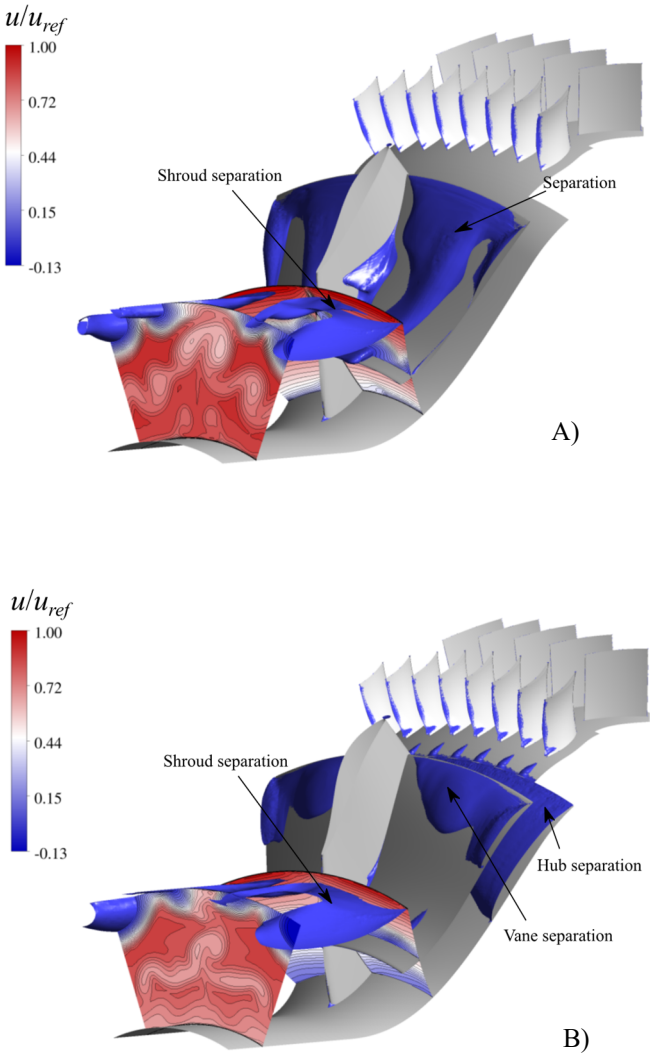

FIGURE 9: NORMALIZED AXIAL VELOCITY COMPUTED FOR THE HEX-1 (A) AND HEX-2 (B) DUCT DESIGN. THE ISO-SURFACE SHOWS REGIONS OF FLOW SEPARATION.

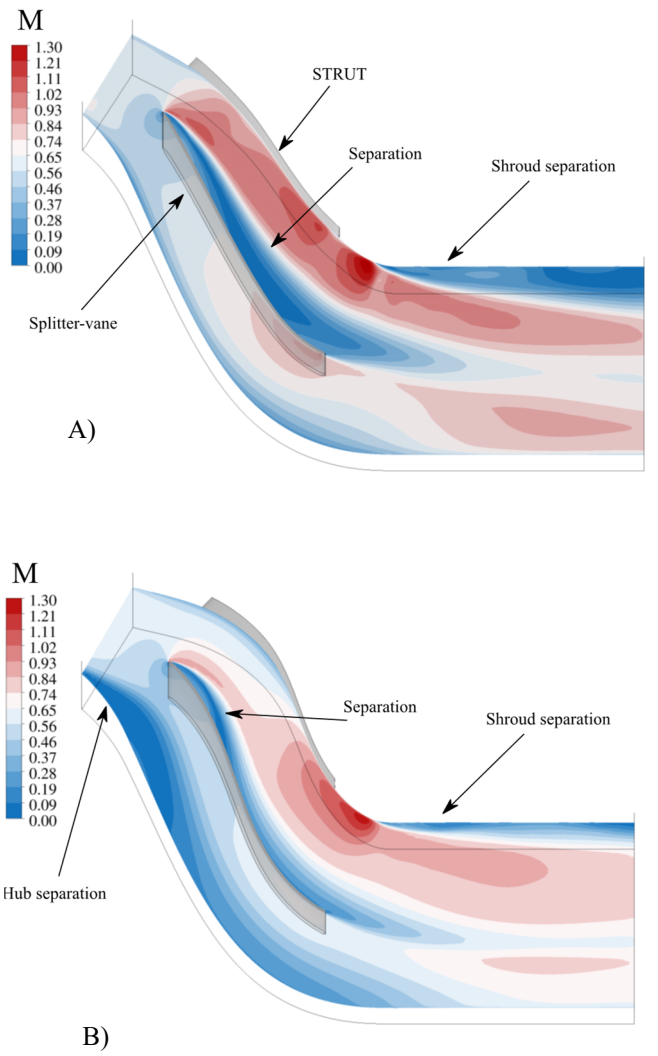

FIGURE 10: MACH NUMBER CONTOUR PLOT AT A CIRCUNFERENTIAL PLANE COMPUTED FOR HEX-1 (A) AND HEX-2 (B) DUCT DESIGN.

Due to the presence of shocks, and the reduction of throughflow area which result from the inclusion of additional surfaces, one aspect to consider in the future is a re-design of the compression system to increase the area at the inlet of the ICD and keep the area ratio between ICD inlet and outlet plane. Increasing the ICD inlet area would result in lower velocities, which would address some of the drawbacks observed in the present paper.

Future work will include more accurate turbulent simulations of the boundary layer in the duct wall regions to improve the prediction of separation and secondary flows. Such models should also be tuned to accurately predict the thermal boundary layers and support the estimation of the thermal performance of the heat exchanger. Ideally, transition models will also be calibrated to ensure an adequate prediction of laminar and turbulent flow regions in the vane. A two-stage low-pressure compressor rig is currently being assembled at Chalmers university to support the validation of such calibrated models. Multi-objective optimizations will also be carried out to support the aero-thermal design of the heat exchanger. The final goal would be the creation of low-order aero-thermal performance models for integration in gas turbine performance tools to support the top-level assessment of cryogenically fueled aircraft concepts.

ACKNOWLEDGEMENTS

The E.U. financially supports this work under the “ENABLEH2 – Enabling cryogenic hydrogen-based CO2 free air transport” Project co-funded by the European Commission within the

Horizon 2020 Programme (2014-2020) under Grant Agreement no. 769241.

REFERENCES

[1] Lejon, M., Grönstedt, T., Glodic, N., Petrier-Repar, P., Genrup, M., and Mann, A., 2017, "Multidisciplinary design of a three stage high speed booster," Proc. ASME Turbo Expo 2017: Turbine Technical Conference and Exposition, ASME.

[2] Grönstedt, T., 2000, Development of methods for analysis and optimization of complex jet engine systems, Ph.D. thesis, Chalmers University of Technology, Göteborg.

[3] Grönstedt, T., Irannezhad, M., Lei, X., Thulin, O., and Lundbladh, A., 2014, "First and Second Law Analysis of Future Aircraft Engines," Journal of Engineering for Gas Turbines and Power, 136(3), pp. 031202-031202-031210.

[4] Grönstedt, T., Xisto, C., Sethi, V., Rolt, A., Rosa, N. G., Seitz, A., Yakinthos, K., Donnerhack, S., Newton, P., Tantot, N., Schmitz, O., and Lundbladh, A., "Ultra Low Emission Technology Innovations for Mid-Century Aircraft Turbine Engines," Proc. ASME Turbo EXPO 2016.

[5] Thulin, O., Petit, O., Xisto, C., Zhao, X., and Grönstedt, T., 2018, "First and Second Law Analysis of Radical Intercooling Concepts," Journal of Engineering for Gas Turbines and Power, 140(8).

[6] Xisto, C., Petit, O., Grönstedt, T., and Lundbladh, A., 2018, "Assessment of CO2 and NOx Emissions in Intercooled Pulsed Detonation Turbofan Engines," Journal of Engineering for Gas Turbines and Power, 141(1).

[7] Zhao, X., Thulin, O., and Grönstedt, T., 2015, "First and Second Law Analysis of Intercooled Turbofan Engine," Journal of Engineering for Gas Turbines and Power, 138(2), pp. 021202-021202-021208.